Proceedings of the ASME/BATH 2019 Symposium on Fluid Power and Motion Control
FPMC2019
October 7–9, 2019, Sarasota, FL, USA

SAND2019-4147C

FPMC2019-1673

DEVELOPMENT OF A LINEAR HYDRAULIC PISTON MOTOR

David W. Raymond[1]
Sandia National Laboratories[2]
Albuquerque, NM

ABSTRACT

Piston motors are widely used in the fluid power industry for high torque applications. Swash-plate and bent-axis motors are the most common configurations. Both types employ a piston group reciprocating in a circular array of cylinders within a rotary barrel. The pistons are displaced in response to the application of fluid power resulting in pressurized inflow or exhaust outflow as the individual cylinders pass across a valve plate concurrently causing the rotary barrel to rotate and generating torque in an output rotor. The reaction of the individual pistons against a swash-plate, or the piston reaction from a bent-axis motor, enable the conversion of reciprocating piston power into continuous rotary shaft power. Development of a high-torque piston motor analog would be beneficial to the drilling industry for downhole applications as high torque is required to penetrate hard rock. However, the centralized distribution of the reciprocating pistons in a rotary barrel encircling the rotor limits torque production as the piston diameter is constrained by the diameter of the motor. A longitudinal piston motor is needed with the pistons axially disposed along the length of the rotor to be applicable to the form factor and performance requirements of drilling operations; the number of pistons is increased in proportion to the required torque.

Work developing technology for a downhole piston motor to enable drilling high strength rock is described. Application of conventional hydraulic piston motor power cycles into longitudinal configurations is detailed. Work is described comprising conceiving downhole piston motor power sections; modeling and analysis of potential solutions; and development and laboratory testing of prototype hardware. The prototype motor hardware is operated on hydraulic power fluids using conventional fluid power sources and load tested using a powder brake dynamometer. A comparison is made between fluid power cycle modeling and test measurements. The longitudinal piston motor configuration can be extended to other applications with large length to diameter ratios where the conversion of fluid power into rotary shaft power with high output torque is needed in slender motor applications.

Keywords: directional drilling, motor, piston motor, longitudinal motor, annular piston, PDM, turbine, drilling, high temperature, vibration mitigation.

Nomenclature

a	piston acceleration
A_0	orifice flow area
A_p	Axial piston pressure area
C_d	orifice discharge coefficient
E_s	Drilling Specific Energy
d	diameter of harmonic drive for torque computation
$d_{b.}$	bit diameter
F_A	axial load applied to the harmonic drive
F_H	Force in horizontal direction
F_R	piston/ring load reaction at the harmonic drive
F_T	Tangential force on Harmonic Drive
F_V	Force in vertical direction
F_z	Force in axial direction
m	number of harmonics per revolution
Mdot	time rate of change of mass in control volume
M	fluid mass in control volume
m_p	mass of the piston
N_m	Rotary Speed
N	Normal force on the harmonic drive and/or ball transfer
p_1	forward motion piston pressure
p_2	backpressure on the piston
P_m	Motor Power

[1] Contact author: dwraymo@sandia.gov

[2] Sandia National Laboratories is a multimission laboratory managed and operated by National Technology and Engineering Solutions of Sandia, LLC., a wholly owned subsidiary of Honeywell International, Inc., for the U.S. Department of Energy's National Nuclear Security Administration under contract DE-NA-0003525. SAND2019-xxxx.

P	Fluid Pressure in control volume
P_b	boundary pressure outside the control volume
Q	Flowrate
r_b	bit radius
r	radius of barrel cam
r	radius of harmonic drive for torque computation
ROP	Rate Of Penetration
s	Circular distance parameter
S	Piston Stroke
t	Time
T	Torque
v	Piston Velocity
V	fluid volume in control volume
V_r	Rock Volume Drilled
z	Piston displacement
<u>Symbols</u>	
β	Rotary angle for piston rise to full stroke
β_f	Bulk Modulus of the fluid
δ	depth of cut
ε	intrinsic specific energy of rock
θ	rotation angle
μ	friction coefficient
ϕ	pressure angle
ρ	fluid density in control volume
ω	rotor speed

INTRODUCTION

Downhole rotation for directional drilling is typically developed with a motor in the bottom hole assembly that develops drilling power necessary to rotate the bit apart from the rotation developed by the surface rig. Existing downhole motors are progressive cavity positive displacement motors and use a helical metal rotor within a helical elastomer stator which limits operation to approximately 350 F (177C). These motors introduce significant lateral vibration to the drilling bottom hole assembly as the rotor follows an eccentric orbit within the motor housing to generate rotation. This rotor motion introduces lateral vibration to the bottom hole assembly contributing to hardware failures and compromising directional drilling objectives. The drilling industry is hampered by drilling dynamic dysfunctions that contribute to reduced performance, hardware failures, and increased drilling costs. Mud turbines operate at higher temperatures but do not have the low speed, high torque performance envelope for use with conventional drill bits. Development of a fit-for purpose downhole piston motor would enable improved directional drilling.

A linear motor concept is evaluated as a viable downhole rotation option. Fundamentally, the concept is a piston motor that relies upon a harmonic drive coupling to convert hydraulically-activated reciprocating piston motion into rotary motion in an output rotor. The concept is physically analogous to hydraulic swash-plate type piston motors that react piston generated forces against an angled swash plate to produce reactive torque in a barrel housing to generate rotary motion. The objective of the work described herein is: 1) Develop technology for a new downhole motor, 2) Design a representative power section and 3) Demonstrate viability with a proof of concept demonstration. This paper describes motor requirements, the hydraulic power cycle, an axial piston solution, computational modeling to support the concept, and a Proof of Concept demonstration.

1. Motor Application Requirements

Drilling performance requirements are needed to quantify specifications for a linear piston motor power section. Theoretical torque specifications can be derived based upon widely-accepted rock-reduction models in the literature using representative properties for typical rock formations. The approach uses a method to predict motor performance requirements for drilling at minimum specific energy. While field drilling rarely proceeds at ideal conditions, the minimum specific energy condition corresponds to maximum drilling efficiency. The derived values correspond to optimum motor performance and should be increased to account for factors such as increased hydrostatic pressure at depth, bit wear, heterogeneous rock, and non-ideal drilling conditions. The specific energy, Es, is the energy required to drill a unit volume of rock where for rotary drilling the energy input is dominated by the rotary work component:

$$E_s = \frac{\text{Rotary Energy Expended Drilling}}{\textit{Unit Rock Volume Removed}} = \frac{\int T\,d\theta}{V_r} = \frac{2\pi T}{\pi r_b^2 \delta} = \frac{2T}{r_b^2 \delta} = \frac{8T}{d_b^2 \delta} \quad (1)$$

where T is the torque required to drive a drill bit, θ is the rotation angle, V_r is the volume of rock removed, r_b is the bit radius, d_b is the bit diameter and δ is the depth of cut per revolution.

Following the method from Detournay [1], the minimum specific energy will approach the *intrinsic specific energy* of the rock formation for "pure cutting" with a polycrystalline diamond compact drag bit – the present-day bit type used for the majority of wellbores drilled. Following Teale [2], it has been observed that the minimum specific energy "is of the order of the compressive strength of the material drilled." Hence, a governing expression for the operational torque, T, for a drag bit to drill a formation of unconfined compressive strength (UCS), at minimum specific energy may be derived from equation (1):

$$T \cong \left(\frac{d_b^2}{8}\varepsilon\right)\delta \quad (2)$$

where ε is the UCS of the rock (psi).

The depth of cut corresponding to a target rate of penetration, ROP and rotary speed, N_m can be computed using the rate equation:

$$\delta = \frac{\text{ROP}}{(N_m)} \quad (3)$$

The rotary power delivered by the motor, P_m, is

$$P_m = \frac{2\pi\, T\, N_m}{(60*550)} \ \text{[hp]} \quad (4)$$

Where N_m is expressed in revolutions per minute. As an example, bit diameters of 4, 6, 8, 10 & 12 inches are evaluated to produce exemplary values. Strength (UCS) values for Berea Sandstone, Arizona Sandstone, Sierra White Granite, and Mississippi Limestone are used as representative values to span the range of UCS values that may be encountered. Rotary speeds are used comparable to what is generally practiced on positive displacement motors. Using these values, tabular data are generated to determine values of $d^2\varepsilon/8$ for several tock types and corresponding torque values. These values are graphically portrayed in Figure 1 and 2.

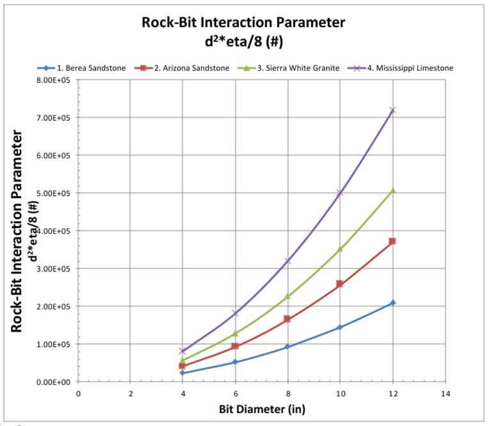

FIGURE 1: ROCK-BIT INTERACTION PARAMETER.

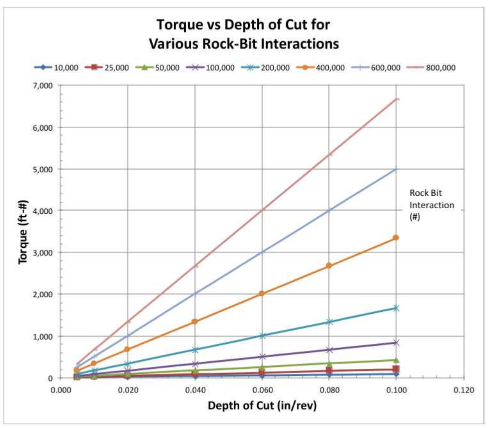

FIGURE 2: TORQUE PREDICTION FOR APPLICATION.

The figures may be used as a "nomograph" to derive the operational torque, subject to known operating conditions, as follows: i) Use Figure 1 to derive the $d^2\varepsilon/8$ term corresponding to the bit diameter and rock type; ii) Use equation (3) to compute the depth of cut per revolution; iii) Use Figure 2 or Equation (2) to derive the torque, T, corresponding to the depth of cut, δ, and $d^2\varepsilon/8$ value; and iv) Use equation (4) to derive the power, P_m, corresponding to the torque, T, and rotary speed, N_m. For a given bit diameter, minimum torque requirements are predicted corresponding to the specified UCS and operating condition. Rotary power output corresponds to the predicted torque and rotary speed condition; hydraulic power input must be greater commensurate with the overall efficiency of the motor.

Another means to identify performance requirements is to conduct a survey of commercially available motors. Of particular interest to this development is a representative 288-56-3 PDM with a 2-7/8 inch motor housing, 5-lobed rotor, 6-lobed stator, and three stages. This motor produces 345 ft-lb at 300 psi pressure differential; the stall torque is 690 ft-lbs at 600 psi differential pressure. This motor will be used as a standard of comparison in the development of a linear piston motor.

2. Conventional Hydraulic Piston Motors

Piston motors are widely used in the mobile hydraulics industry. The general configuration is shown in Figure 3. It consists of an array of pistons in individual cylinders symmetrically disposed around the central axis of a cylindrical barrel. The piston motor generates rotary motion and output torque in response to pressurized fluid conveyed across the valve plate to the individual pistons. As the cylindrical barrel rotates, the individual cylinders periodically pass over the intake and discharge ports on the valve plate. As the individual pistons experience inlet pressure, the piston slipper reacts against a front swash plate. Since the swash plate is inclined at an angle, α_b, with respect to the central shaft the pistons will experience harmonic motion as the cylindrical barrel rotates. Since the slipper reacts against the swash plate at an angle, a side load is produced that acts on the cylindrical barrel inducing rotation. The motion of the cylindrical barrel is coupled to the output shaft of the machine to deliver rotary speed and motive torque for the application. Figure 4 describes rotor torque generation in the piston motor.

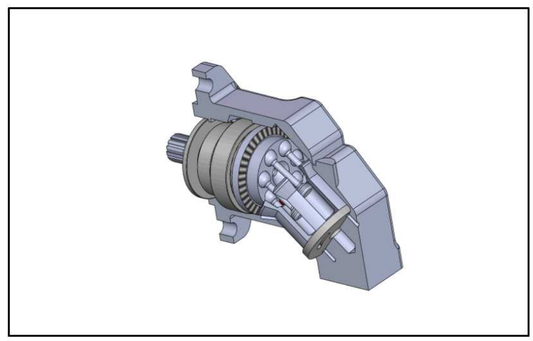

FIGURE 3: CONVENTIONAL HYDRAULIC PISTON MOTOR.

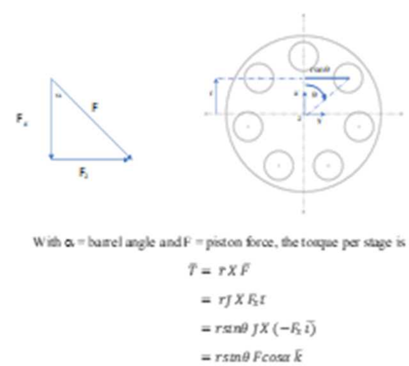

FIGURE 4: METHOD OF TORQUE GENERATION.

3. Longitudinal Piston Motor Concept

3.1. Overview

The objective of this work is to develop a prototype power section that enables a longitudinal form factor of the typical hydraulic piston motor shown in Figure 3. Following the analog of the hydraulic piston motor, it should include the following power section design features.

- The fluid power cycle should generate piston oscillation by hydraulic flow through the power section. This will require alternating pressure on the piston lands for reciprocation and will require the valves to be synchronized to the piston motion.
- A harmonic drive coupling must convert axial piston force and motion to rotor torque and rotation.
- It will require multiple pistons for continuous rotation to overcome the dwell points, or motion reversals of the pistons. Multiple pistons will additionally be required for adequate torque generation.
- The overall design intent must accommodate: 1) fluid leakage around the piston section (no seals), 2) Low friction surfaces at the piston interfaces to reduce parasitic losses, 3) A removable rotor assembly for servicing, 4) case/rotor design integration, 5) pressure/exhaust manifold integration, and 6) piston motion / valve port integration.

An axial piston motor configuration has been conceived, designed and developed for a longitudinal piston motor and is the subject of the balance of this paper.

3.2. Component Descriptions

The form factor of a downhole piston motor excludes use of the general design configuration used in a conventional piston motor as the piston forces would be inadequate to develop sufficient torque to be comparable to the requirements presented above. Accordingly, the hydraulic piston motor design arrangement must be linearized by sequential arrangement of piston motor modules that work collectively to generate rotation and torque analogous to hydraulic piston motors except the pistons are not symmetrically distributed around a common output rotor but rather linearly distributed along the axis of the power section. This allows the major dimension of the piston to approach the diameter of the motor housing giving rise to higher net torque. Such a linear axial piston motor module in shown in Figure 5 and performs the speed and torque generation function of a single piston within a conventional hydraulic motor. Other configurations can be conceived as described in the referenced patents. A linear array of these modules may be serially connected to a common output shaft to produce an entire power section for a full motor. The axial piston motor module concept in Figure 5 includes several major assemblies: Housing, Liner, Rotor and Exhaust Manifold, Valves and Valve Block, Piston, Ball Transfer and Harmonic Drive. These assemblies comprise the linear piston motor concept with the following attributes.

Housing - The housing is the body of the motor and protects the inner components from the return flow in the annulus.

Liner - A liner is the motor interface to the housing. It allows reactive torque in the liner to be transferred to the housing. It also provides features for fluid conveyance as needed for fluid power conversion.

FIGURE 5: AXIAL PISTON MOTOR MODULE[3].

Rotor/Exhaust Manifold – The rotor is the main fluid conduit through the motor and must deliver pressurized flow to the piston and collect exhaust when discharged. It is also the member that carries the shaft power from the individual modules comprising the power section to the balance of the motor. Figure 6 & Figure 7 show the rotor with an exhaust manifold within it to collect and transfer exhaust flow to the end of the power section. The integration of the exhaust manifold with the rotor must keep the flows separated until the power fluid has been delivered to all chambers comprising the power section.

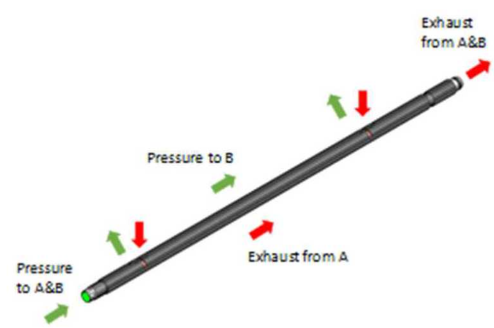

FIGURE 6: ROTOR WITH CENTRALIZED MANIFOLD.

Valve Block & Valves - Like conventional hydraulic motors, the longitudinal motor concept employs rotary valves that selectively pressurize and exhaust piston chambers during rotor rotation. The function of the valve block is to convey power fluid to the piston chamber to act on the piston. The valves are keyed to the rotor with pressurization and discharge ports that are synchronized with piston reciprocation. The valve ports and passages are specified to convey required flowrates to support piston extension and retraction.

Piston - The hydraulic energy in the pressurized drilling fluid is converted to kinetic energy in the piston. The piston reacts

[3] U.S. Patent 9,447,798B1 from U.S. Patent Application No. 14/209,840, filed 3/13/2014; CIP of U.S. App. No. 14/298,377, filed 05/05/2014 and U.S. Provisional Patent Application No. 62/142,837, filed 4/3/2015 and U.S. Patent App. No. 15/090,282 - Modular Fluid Powered Linear Piston Motors with Harmonic Coupling and U.S. Patent App. No. 62569074 - Fluid-Powered Linear Motor with Rotary Pistons and Motion Rectifier.

against a barrel cam during its stroke to convert piston kinetic energy to output rotor rotational energy. The interface between piston and rotor requires high strength ball transfers to facilitate conversion of piston force into rotor torque. The piston seals against the liner and reciprocates in response to differential pressure on its lands. The piston reacts against the harmonic drive to develop torque in the output rotor. Like in the hydraulic analog, the piston must react against an inclined plane to develop a lateral force component to produce torque in the output rotor.

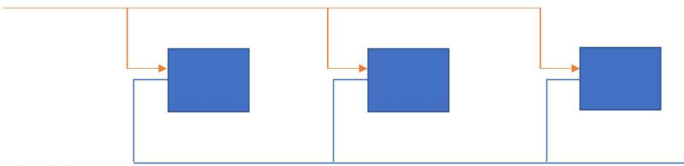

FIGURE 7. PRESSURE AND EXHAUST MANIFOLD.

Ball transfer – The ball transfer takes the place of the slipper foot in the hydraulic piston motor. However, rather than sliding across the inclined plane as the slipper foot does on the swash plate, the ball transfer rolls on the harmonic drive. At the piston interface, the ball rides in a special seat to reduce rolling friction at the piston interface.

Harmonic Drive - The hydraulic energy is converted to kinetic energy in the piston that must be converted to motive torque in the rotor. This is accomplished in the axial piston motor module shown in Figure 5 using a barrel cam – the central feature of the Harmonic Drive. The barrel cam is preferentially specified to generate torque in the output rotor. The harmonic drive is a cylindrical cam, sometimes referred to as a drum or barrel cam, manufactured to produce the desired displacement response in the piston with rotor turning angle. As described in Figure 8, the barrel cam is characterized by a cut in the circumferential surface of the harmonic drive. This feature is mathematically specified so that a cam follower will produce desired motion. The cam follower can be specified using a harmonic, a cycloid, or polynomial functions (Mabie and Ocvirk, 1978).

3.3. Kinematic Response

Assuming a harmonic function, the follower (piston) displacement is

$$z = \frac{S}{2}\left(1 \ - \cos\left(\frac{\pi\theta}{\beta}\right)\right) = \frac{S}{2}(1 \ - \cos(m\theta)) \qquad (5)$$

where z is the piston displacement, S is the Stroke, and m is the number of harmonics per revolution with $m = \frac{\pi}{\beta}$ where β is the angular rotation to full stroke S. For a single harmonic per revolution, m= 1 and β=π. Likewise, for two harmonics per revolution, m=2 and β=π/2, etc.

The inclination or pressure angle, ϕ, throughout the cycle is also of interest as this will influence the conversion of piston thrust to torque. As shown in Figure 9, the inclination angle is $\tan^{-1}(\frac{dz}{ds})$. Using s = rθ for the circular distance on the barrel at the barrel cam radius, r, then

$$\frac{dz}{ds} = \frac{dz}{d\theta}\frac{d\theta}{ds} \qquad (6)$$

$$\emptyset = \tan^{-1}[\frac{\pi S}{2\beta r}\sin(\frac{\pi\theta}{\beta})] = \tan^{-1}[\frac{mS}{2r}\sin(m\theta)] \qquad (7)$$

Note there is a preferred ratio of stroke to radius for a given harmonic drive to produce favorable pressure angles in the harmonic motion response.

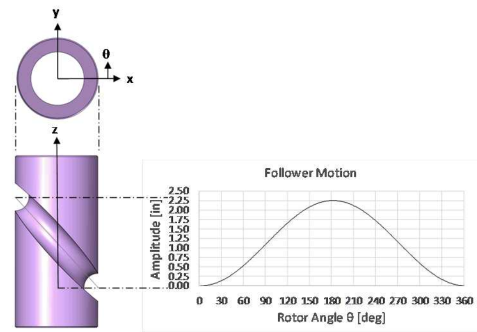

FIGURE 8: BARREL CAM CONSTRUCTION IMPARTING HARMONIC MOTION TO A FOLLOWER.

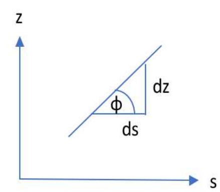

FIGURE 9: PRESSURE ANGLE FOR BARREL CAM.

The piston velocity, v, and acceleration, a, are known from the cam follower motion (Figure 10):

$$v = \frac{dz}{d\theta} = \frac{\pi S}{2\beta}\left(sin\frac{\pi\theta}{\beta}\right) = \frac{mS}{2}(\sin(m\theta\,)) \qquad (8)$$

$$a = \frac{dv}{d\theta} = \frac{\pi^2 S}{2\beta^2}(cos\frac{\pi\theta}{\beta}) = \frac{m^2 S}{2}(cos(m\theta\,)) \qquad (9)$$

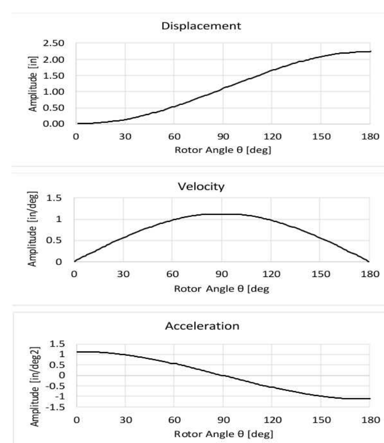

FIGURE 10: PISTON DISPLACEMENT, VELOCITY AND ACCELERATION FROM BARREL CAM HARMONIC MOTION.

3.4. Piston Force Balance

The force balance on the piston in Figure 11 is

$$\sum F_z = p_1 A_p - p_2 A_p - F_R - m_p \ddot{z} = 0 \qquad (10)$$

where p_1 is the forward motion piston pressure, p_2 is the backpressure on the piston, F_R is the load reaction at the harmonic drive, m_p is the mass of the piston, A_p is the piston area, and piston friction is neglected, then

$$F_R = A_p(p_1 - p_2) - m_p \ddot{z} \qquad (11)$$

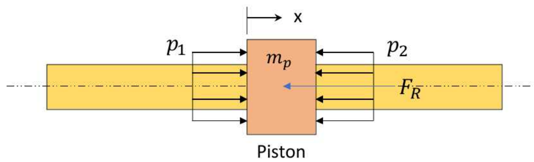

FIGURE 11: PISTON FREE BODY DIAGRAM.

3.5. Rotor Torque Generation

Following the example of Shigley and Mitchell for the Mechanics of Power Screws, imagine an infinitesimal length of the single harmonic track that is unrolled, as shown in Figure 12. One edge of the track will form a hypotenuse of a right angle with a corresponding pressure angle, ϕ. The axial force, F_A, applied to the harmonic drive is transmitted from the ball transfer (i.e., equal and opposite to F_R). A load F_T acts on the contact point to resist lowering the load F_A along the track. This load is produced by the resistive torque load on the rotor assembly.

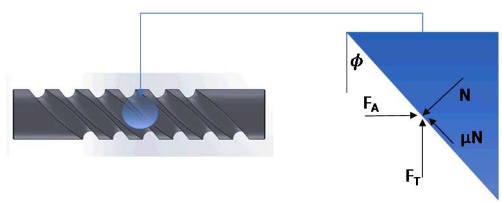

FIGURE 12: FORCE BALANCE AT THE HARMONIC DRIVE/BALL TRANSFER INTERFACE.

Summing forces in the horizontal direction and solving for N:

$$\sum F_H = F_A - N\cos\phi - \mu N \sin\phi = 0$$

$$N = \frac{F_A}{\cos\phi + \mu \sin\phi} \qquad (12)$$

And in the vertical direction and solving for F_T:

$$\sum F_V = F_T - N\sin\phi + \mu N\cos\phi = 0$$

$$F_T = N(\sin\phi - \mu\cos\phi) \qquad (13)$$

Combining to eliminate the normal force N and dividing top and bottom by cosϕ:

$$F_T = F_A \frac{(\sin\phi - \mu\cos\phi)}{(\cos\phi + \mu\sin\phi)}$$

$$F_T = F_A \frac{(\tan\phi - \mu)}{(1 + \mu\tan\phi)} \qquad (14)$$

The torque on the harmonic drive due to the ball reaction F_T is $T = F_T\, d/2 = F_T\, r$ where d and r are the corresponding diameter and radius at the ball contact. The torque on the harmonic drive is:

$$T = F_T r = F_A r \frac{(\tan\phi - \mu)}{(1 + \mu\tan\phi)} \qquad (15)$$

4. Fluid Power Cycle

A control volume of the piston bore is used to address the coupling between the power fluid mechanics and the reciprocating pistons, and investigate influence of valve geometry and timing on motor performance. This will prescribe the pressure variation with rotor rotation within the piston chamber and is used to address a force balance on the piston and determine its influence on rotor torque generation. The governing equations are developed and then used in a computational code to predict results.

4.1. Control Volume Analysis

A control volume is defined for the piston bore as shown in Figure 13. The instantaneous mass within the piston bore is

$$M = \rho V \qquad (16)$$

where M, ρ & V are the fluid mass, density and volume of the control volume, respectively.

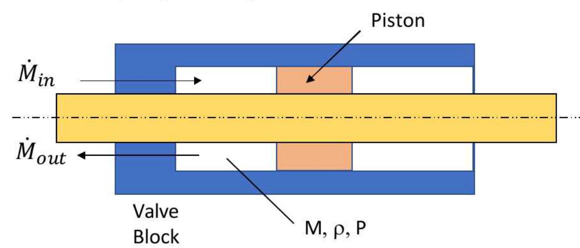

FIGURE 13: CONTROL VOLUME OF THE PISTON BORE.

Following the method of Manring for conventional piston motors [4], the fluid mass time rate of change is

$$\frac{dM}{dt} = \frac{d\rho}{dt}V + \rho\frac{dV}{dt} \qquad (17)$$

For a mass flow rate $\dot{m}$, and defining Q as the flow rate, then for conservation of mass

$$\frac{dM}{dt} = \rho Q = \dot{M}_{in} - \dot{M}_{out} \qquad (18)$$

From the definition of Bulk Modulus,

$$\beta_f = \rho\frac{dP}{d\rho} \qquad (19)$$

where β_f is the bulk modulus of the fluid and P is the fluid pressure, then,

$$\frac{dM}{dt} = \rho Q = \frac{\rho}{\beta_f}\frac{dP}{dt}V + \rho\frac{dV}{dt} \qquad (20)$$

Solving for the pressure change,

$$\frac{\rho}{\beta_f}\frac{dP}{dt}V = \rho Q - \rho\frac{dV}{dt} = \rho\left(Q - \frac{dV}{dt}\right) \qquad (21)$$

$$\frac{dP}{dt} = \frac{\beta_f}{V}\left(Q - \frac{dV}{dt}\right) \qquad (22)$$

With θ as the rotor angle, and ω as the rotor speed, then using $\omega = \frac{d\theta}{dt}$ and applying the chain rule as $\frac{dV}{dt} = \frac{dV}{d\theta}\frac{d\theta}{dt}$, then the pressure in the chamber as a function of rotary angle is

$$\frac{dP}{dt} = \frac{dP}{d\theta}\frac{d\theta}{dt} = \frac{\beta_f}{V}\left(Q - \frac{dV}{d\theta}\frac{d\theta}{dt}\right) \tag{23}$$

and

$$\frac{dP}{d\theta} = \frac{\beta_f}{V}\left(\frac{Q}{\omega} - \frac{dV}{d\theta}\right) \tag{24}$$

This formulation shows the flowrate in and out of the control volume must be proportional to rotary speed as the piston extends and retracts to change the size of the control volume. If proportional flow is maintained, then the difference function may be approximately zero and the pressure variation will not change significantly with rotation. It also shows the flowrate generally must follow the velocity distribution as the dV/dθ term depends upon the piston speed. Finally, this function shows the ratio of the bulk modulus of the fluid to the fluid volume will act as a gain on this difference magnifying the pressure gradient during the piston reciprocation cycle. This gain is particularly influential at minimum chamber volume.

4.2. Flowrate

The flowrate is determined using the orifice equation governing flow through the valve block assembly based upon the pressure in the control volume:

$$Q = C_d A_0 \sqrt{2\left|\frac{P_b - P}{\rho}\right|} \tag{25}$$

Where C_d is an orifice discharge coefficient, P_b is the boundary pressure outside the control volume, A_o is the orifice flow area and as before P is the pressure in the control volume and Q is the flowrate.

4.3. Computational Modeling Results

The physics coupling hydraulic fluid power, piston oscillation, and rotor shaft power are engineered using a fluid-structure interaction computational model. An integration scheme is used to account for the dP/dθ term. Assuming a three-module motor at constant rotor speed, the overall response is shown in Figure 14 & Figure 15 for a three-module motor with 2-5/8 inch x 1-3/8 diameter pistons.

Of interest is the pressure profile as a function of rotor angle. This shows for proper design, the pressure in the control volume may be fairly constant during piston extension and retraction. While the oscillations at the end point are dependent upon the accuracy of the integration scheme, the valves must be properly designed to manage pressure pulsations at the ends of the stroke. This result of near constant pressure allows for high torque production as the piston/harmonic drive combination passes through maximum pressure angle. The bottom panels in Figure 15 show the required flowrate for a 100 RPM motor speed and the resulting output torque at a 600 psi pressure differential across the pistons.

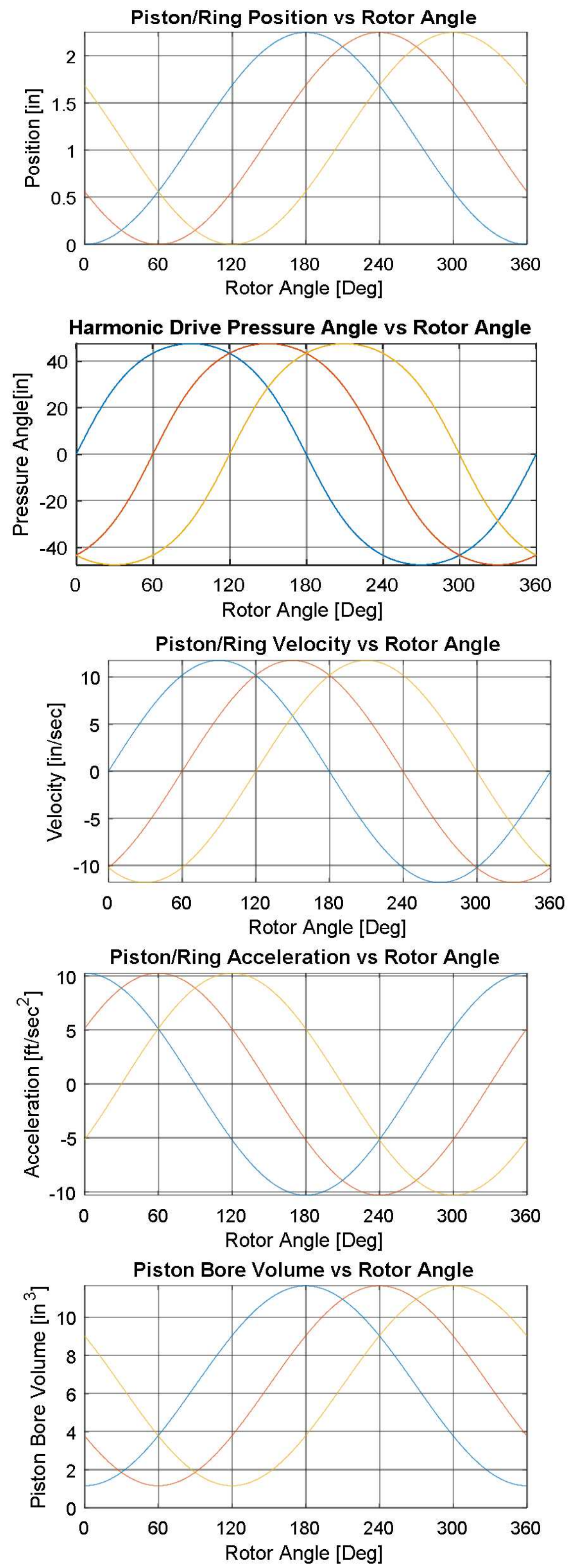

FIGURE 14: FLUID POWER CYCLE MODELING KINEMATIC RESULTS (A-E, TOP TO BOTTOM, RESPECTIVELY)

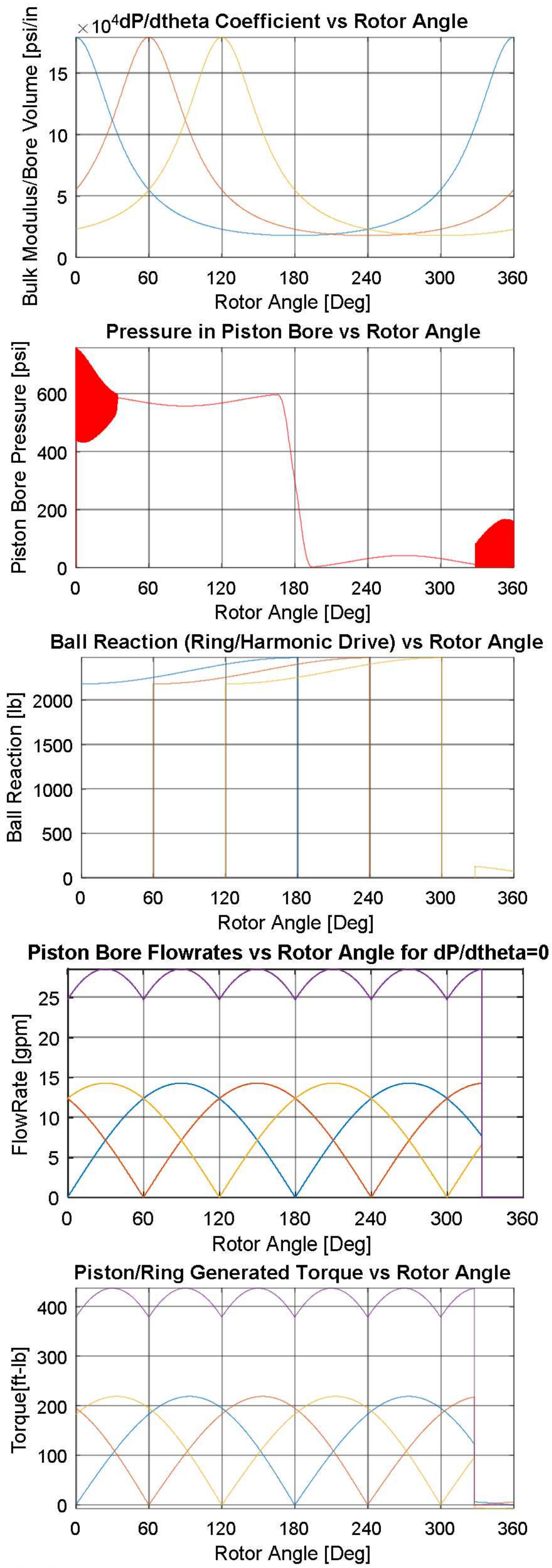

FIGURE 15: FLUID POWER CYCLE MODELING DYNAMIC RESULTS (A-E, TOP TO BOTTOM, RESPECTIVELY)

5. Static Load Qualification Testing

Quasi-static loads are applied using test fixtures to qualify components for service. The overall assembly was load tested to qualify the assembly for Proof of Concept (POC) testing and evaluate the pressure/torque relationship of the overall assembly. The Linear Piston Motor module is assembled and loaded into a static load test fixture (Figure 16) to qualify for operational thrust loads generated by the pressure system. As a hydraulic cylinder applies an axial load to the piston assembly to simulate a pressure load, the applied load is measured at the opposite end of the assembly using a bi-axial thrust/torque load cell. The fixture includes a thrust bearing reaction internal to the assembly that allows the reactive torque in the motor assembly to be measured independently of the axial thrust. The relationship between applied force and measured torque is shown in Figure 17 for several pressure angles. This compares with the predictions of Eq. (15) predicting torque as a function of piston thrust load.

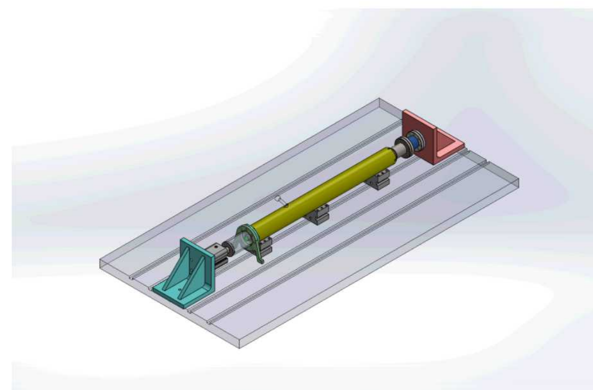

FIGURE 16: PROTOTYPE MOTOR MODULE IN LOAD TEST FIXTURE.

Load Testing Results

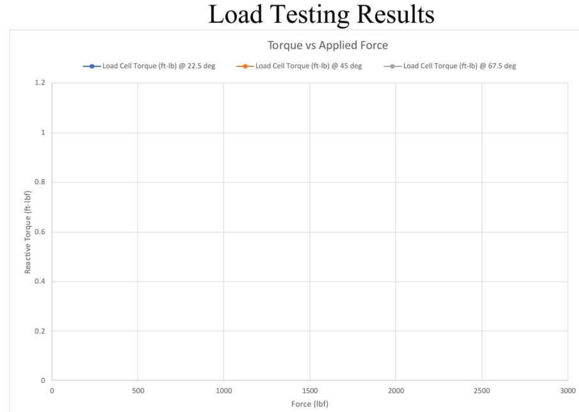

FIGURE 17: REACTIVE TORQUE FROM HARMONIC DRIVE VERSUS PISTON APPLIED LOAD [DATA TO BE ADDED].

6. Dynamometer Test Station

A Dynamometer Test Station (Figure 18) is used to provide a resistive load to the test motor to simulate the downhole drilling environment. The axial piston motor is installed in a pressure vessel (Figure 19) and powered by a hydraulic power unit

(Figure 20). The dynamometer is connected to a water supply from the chiller to transfer the rotary power absorbed from the motor into heat. Other equipment includes:

Table - A table manufactured from structural steel tubing is used to support the test articles and dynamometer.

Pressure Vessel - A custom-designed pressure vessel is used to house the linear piston motor. The reactive torque from operation is supported by the pressure vessel stand to that the pressure vessel is not subject to torque loading.

Rotating Head - A rotating head is used to transmit rotation out of the pressure vessel while maintaining a high-pressure seal within the pressure vessel.

Swivel - A swivel is used to convey hydraulic fluid power from of the drive line while transmitting rotational power to the drive train assembly for absorption by the dynamometer.

Drive Train Assembly - A drive train assembly is used to connect the test motor to the dynamometer input shaft. A conventional hydraulic piston motor is used to rotate a drive pulley that is connected to a flywheel through a positive belt drive assembly. The drive train assembly allows continuous rotation of the rotor/flywheel system as the piston on the test motor goes through motion reversals. The ratio of the drive train pulleys allows for a 4:1 drive ratio. A spider coupling is used to connect the drive train rotor to the dynamometer input shaft.

Dynamometer - The dynamometer consists of a powder brake dynamometer (Magtrol P/N 4PB15), DSP6001 dynamometer controller, TSC 401 Torque- Speed conditioner, and DES Power Supply. The load absorbed by the dynamometer is controlled thru the M-Test 5.0 software interface provided by Magtrol. This software generates control commands to the dynamometer controller/power supply to establish braking conditions developed within the dynamometer. The Magtrol system is connected to the Data Acquisition system via the TSC 401 Torque- Speed conditioner.

Data Acquisition - A desktop computer-based data acquisition system is used to monitor the operating conditions of the dynamometer test station. The system monitors the torque and speed conditions of the dynamometer in addition to various other parameters throughout the system.

Sensors - A variety of sensors are deployed throughout the system to monitor performance including pressure gages, flow meters, and temperature sensors.

Hydraulic Power Unit - A hydraulic power unit is used to generate fluid power to drive the piston motor. It is a 50 hp unit that produces 50 GPM at 3000 psi.

Distribution Piping - Stainless steel tubing and hydraulic hose are used to route hydraulic fluid supply and return flows from the hydraulic power unit to the dynamometer table.

Chiller - The chiller is used to transfer the heat absorbed from the dynamometer into the ambient air. The chiller is connected to the dynamometer and power supply using flexible hose. The chiller includes an internal pump that provides flow to the dynamometer.

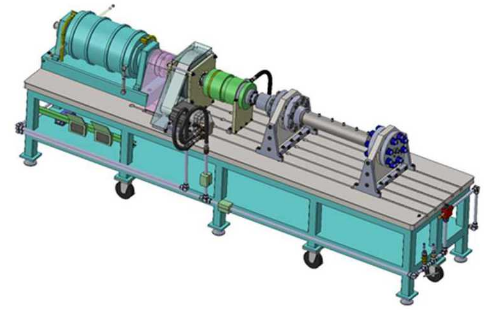

FIGURE 18: DYNAMOMETER TEST STATION.

7. Proof of Concept (POC) Demonstration and Laboratory Testing

7.1. Test Description

The axial piston motor is run on the dynamometer at varying flowrates (Figure 21) and braking torques (Figure 23) to simulate the rock drilling load.

7.2. Results

The operational performance of the axial piston motor is summarized in Figure 22 & Figure 24 below.

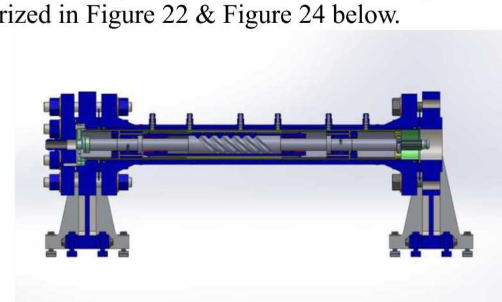

FIGURE 19: AXIAL PISTON MOTOR MODULE IN DYNAMOMETER TEST STATION PRESSURE VESSEL / TEST CHAMBER.

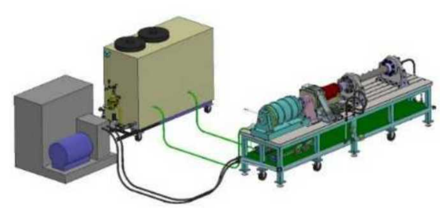

FIGURE 20: DYNAMOMETER TEST STATION WITH HPU AND CHILLER.

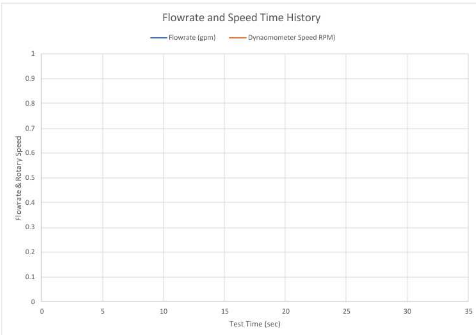

FIGURE 21: FLOWRATE AND DYNAMOMETER ROTARY SPEED DURING TEST [DATA TO BE ADDED].

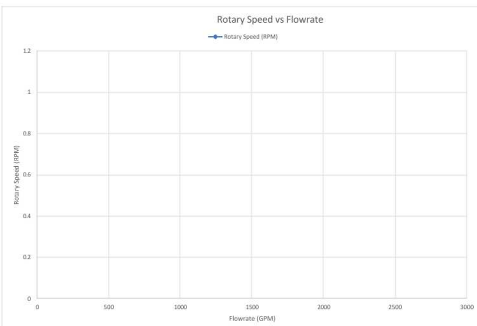

FIGURE 22: AVERAGE DYNAMOMETER ROTARY SPEED OVER RANGE OF FLOW CONDITIONS [DATA TO BE ADDED].

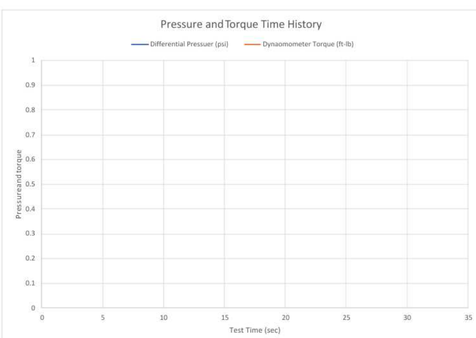

FIGURE 23: PRESSURE AND DYNAMOMETER TORQUE DURING TEST [DATA TO BE ADDED].

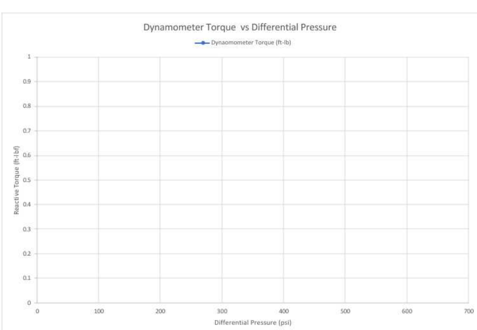

FIGURE 24: AVERAGE DYNAMOMETER TORQUE OVER RANGE OF PRESSURE CONDITIONS [DATA TO BE ADDED].

8. Conclusions

A linear piston motor can be designed with a firm understanding of the principles affecting operation including the fluid power cycle in cooperation with piston reciprocation, ball transfer reactions, and rotor torque generation; quasi-static load testing validates an understanding of the piston/ball transfer/barrel cam geometry; Proof of Concept testing on a dynamometer confirms the operation of a single module. A motor can be made from multiple modules that meets overall design requirements, as per the computational modeling and preliminary test results presented.

ACKNOWLEDGEMENTS

This work was supported by the U.S. DOE/EERE Geothermal Technologies Office. The author gratefully acknowledges the contributions of his colleagues at Sandia, especially Doug Blankenship, Elton Wright, Jeff Greving, William Radigan, Dennis King, Jiann-Cherng Su, Michelle Williams, and Joseph Pope. Sandia National Laboratories is a multimission laboratory managed and operated by National Technology and Engineering Solutions of Sandia, LLC., a wholly owned subsidiary of Honeywell International, Inc., for the U.S. Department of Energy's National Nuclear Security Administration under contract DE-NA-0003525. SAND2019-xxxx.

REFERENCES

[1] Detournay, E., Defourny, P., "A Phenomenological Model for the Drilling Action of Drag Bits," Int. J. Rock Mech. Min. Sci. & Geomech. Abstr., Vol. 29, No.1, (1992) pp. 13-23.

[2] Teale, R., "The Concept of Specific Energy in Rock Drilling," Int. J. Rock Mech. Mining Sci., Vol. 2, (1965), pp. 57-73.

[3] Mabie, H.H., and Ocvirk, F. W., "Mechanisms and Dynamics of Machinery," 3rd Ed., Wiley & Sons, (1978), pp. 45-60.

[4] Manring, N.D., "The Torque on the Input Shaft of an Axial-Piston Swash-Plate Type Hydrostatic Pump," ASME Journal of Dynamic Systems, Measurement and Control, Vol. 120, (1998).

[5] Robello, Samuel, "Positive Displacement Motors", Sigmaquadrant, (2015).

[6] Shigley, J.W., and Mitchell, L.D., "Mechanical Engineering Design, 4th Ed., McGraw-Hill, (1983), pp.362-366.

[7] U.S. Patent 9,447,798B1 from U.S. Patent Application No. 14/209,840, filed 3/13/2014; CIP of U.S. App. No. 14/298,377, filed 05/05/2014 and U.S. Provisional Patent Application No. 62/142,837, filed 4/3/2015 and U.S. Patent App. No. 15/090,282 - Modular Fluid Powered Linear Piston Motors with Harmonic Coupling and U.S. Patent App. No. 62569074 - Fluid-Powered Linear Motor with Rotary Pistons and Motion Rectifier.